

Supporting Information:

Titin-Based Nanoparticle Tension Sensors Map High-Magnitude Integrin Forces within Focal Adhesions

Kornelia Galior,[†] Yang Liu,[†] Kevin Yehl,[†] Skanda Vivek,[‡] and Khalid Salaita^{*,†}

[†] Department of Chemistry, Emory University, 1515 Dickey Dr., Atlanta, GA 30322, United States

[‡] Department of Physics, Emory University, 400 Dowman Drive, Atlanta, GA 30322, United States

Corresponding Author

*k.salaita@emory.edu

Materials and Methods

Reagents. The fluorescent dye dibenzocyclooctyne-Cy3 (DBCO-Cy3), dithiothreitol (99%, DTT), (3-aminopropyl) trimethoxysilane (97%, APTMS), 4-(2-hydroxyethyl)piperazine-1-ethanesulfonic acid (≥99.5%, HEPES), potassium phosphate monobasic (≥99.0%), Y-27632 dihydrochloride (>98%), and Hank's balanced salts (#H1387) were purchased from Sigma-Aldrich (St. Louis, MO). For ACP-tag labeling, CoA 488 and SFP synthase were purchased from New England BioLabs (Ipswich, MA) and were used according to manufacturer protocol. The Slide-A-Lyzer™ Dialysis Cassettes and the fluorescent dyes: Alexa647 N-hydroxysuccinimidyl ester and Alexa647 DIBO alkyne were purchased from Life Technologies (Grand Island, NY). 4-Azido-L-phenylalanine was purchased from Chem-Impex International (Wood Dale, IL). Ni-NTA Agarose (#30210) was purchased from Qiagen (Valencia, CA). Number two glass coverslips, 24-well, and 96-well plates were purchased from Fisher Chemical & Scientific (Pittsburg, PA). Dimethyl sulfoxide (99.5%, DMSO) and sodium bicarbonate were purchased from EMD chemicals (Philadelphia, PA). P2 gel size exclusion beads were purchased from BioRad (Hercules, CA). DI water was obtained from a Nanopure water purification system equipped with a UV sterilization unit with a resistivity of 18.2 MΩ.

Cell Culture. Rat embryonic fibroblasts (REFs) were cultured in DMEM (Mediatech) supplemented with 10% FBS (Mediatech), penicillin G (100 IU ml⁻¹, Mediatech) and streptomycin (100 µg ml⁻¹, Mediatech) at 37 °C in the presence of 5% CO₂. On the day of the experiment, cells were plated on the functionalized coverslips in a custom-made chamber with cell media containing 0.5% FBS to minimize nonspecific absorption of serum proteins. Cells were allowed to adhere for: ~30 minutes on RGD-ACP(A488)-I27 and RGD-Cy3-I27 functionalized surfaces; ~2 h on clamped RGD-Cy3-I27_{G32C-A75C} functionalized surfaces; and 3 h on RGD-sfGFP-I27 functionalized surfaces. Kinetic experiments were conducted with adhered cells that were allowed to spread on the surface for 2 h. To initiate the kinetics measurements, DTT was added to the chamber ($t=0$) and the timelapse video (300 ms exposure time) was collected with the following acquisition frequency: 30 s per frame at 0.25 mM DTT, 15 s per frame at 2.5 mM DTT, 10 s per frame at 5 mM DTT, 3 s per frame at 12.5 mM and 2 s per frame at 25 mM DTT.

Transfection. REF cells were transfected with mCherry-lifeact and GFP-Pax (Addgene plasmid # 15233) using Lipofectamine® LTX (Life Technologies) following the manufacturer protocols. In short, 1 µg of DNA was mixed with Lipofectamine® LTX and Plus™ Reagent per well in a 24-well plate and incubated for 48 h prior to imaging.

Antibody blocking. REF cells were incubated with monoclonal antibodies selective for $\alpha_5\beta_1$ (MAB1969, Millipore) and $\alpha_v\beta_3$ (MAB1976, Millipore) at 10 µg/ml for 30 min. Additionally, each sensor surface prior to REF cell incubation were treated with 10 µg of antibody to ensure complete inhibition of $\alpha_5\beta_1$ and $\alpha_v\beta_3$.

Protein Engineering. I27 based constructs were designed with N-terminal ligand (either TVYAVTGRGDSPASSAA or FN type III domains 9-10) and two C-terminal cysteines for attachment onto AuNPs. For kinetic studies, we used a Cys free I27 variant protein in which Cys⁴⁷ and Cys⁶³ were mutated to Ala. A disulfide bond was introduced into this variant by mutating Gly³² and Ala⁷⁵ to cysteines. The proteins were purified by Ni²⁺ affinity chromatography and stored at -80 °C in 0.1 M potassium phosphate buffer (pH 7.4) prior to use.

Protein Expression with UAA incorporation. The pET22b plasmid encoding MTFM with a TAG codon was co-transformed with pEVOL-pAzF plasmid into electrocompetent BL21(DE3) *E. coli* cells². Cells were grown at 37 °C in the presence of ampicillin, chloramphenicol, and 0.2% glucose to an optical density (OD) of 0.2, at which 1 mM of 4-azido-L-phenylalanine was added. At an OD of 0.4, L-arabinose was added to a final concentration of 0.02% (w/v) and at an OD of 0.8, isopropyl β-D-1-thiogalactopyranoside (IPTG) was added to a final concentration of 1 mM. Cells were shaken for 16 h at 30 °C and purified using His tag chromatography.

Dye labeling. Protein sensors expressing an ACP-tag were incubated with CoA 488 for 1 h at 37 °C, followed by overnight incubation at 4 °C. Protein sensors expressing pAzF were incubated with either DBCO-Cy3 or DIBO-A647 for 1 h at 37 °C, followed by overnight incubation at room temperature. All protein sensors were purified using P2 gel size exclusion beads and the labeling ratio was quantified by UV-Vis absorption (NanoDrop).

AuNP Surface Preparation. Glass coverslips were piranha etched for 30 min, functionalized with an APTMS solution in acetone for 1 h and thermally annealed at 80 °C for 30 min. Subsequently, the surfaces were passivated with 5% (w/v) mPEG-NHS and 0.5% (w/v) lipoic acid-PEG-NHS in 0.1 M fresh sodium bicarbonate overnight at 4 °C. After passivation, 12 nM of AuNPs (diameter = 9 nm) were incubated onto the surface for 30 min.

AFM imaging. The atomic force microscope was attached to an anti-vibration stage (Asylum Research, CA). The force constant of the silicon cantilever (MikroMasch) used in our experiment was 5.4-16 N/m. AuNPs (9 nm) were immobilized onto the surface for 30 min and the surfaces were scanned at a rate of 1 Hz at room temperature. Images were generated using IgorPro.

Optical microscopy. A Nikon Eclipse Ti microscope driven by the Elements software package was used for imaging. The microscope is equipped with a TIRF launcher with three laser lines: 488 nm (10 mW), 561 (50 mW), and 638 nm (20 mW), an intensilight Epifluorescence source (Nikon), an Evolve electron multiplying charge coupled device (EMCCD camera, Photometrics), and a CFI Apo 100x (NA 1.49) objective (Nikon). The microscope includes the following filter cubes TIRF 488, TIRF 640, FITC, TRITC, and RICM (reflection interference contrast microscopy) purchased from Chroma (Bellows Falls, VT). The microscope is also equipped with the Nikon Perfect Focus System that maintains focus during timelapse imaging experiments.

Data Analysis. Fluorescence analysis was performed using ImageJ (National Institutes of Health) and Origin software (OriginLab Corporation). Based on Witta *et al.*, we used the following relation to determine the rate of unfolding: $k(F) = A \exp((F\Delta x_r - E_a)/k_B T)$. The pre-exponential factor $A = 1.3 \times 10^{12} \text{ M}^{-1} \text{ s}^{-1}$, the distance to the transition state for the reaction, $\Delta x_r = 0.34 \text{ \AA}$, and the activation energy (E_a) for the disulfide reduction at $F=0$ was set to 65 kJ/mol. Fernandez *et al.* determined different values for E_a , Δx_r and A using different experimental conditions in three reports^{1, 3} (Supplementary Table 1). In our study, we decided to use the values determined from Witta *et al.*¹ because these are the only experiments where $k(F)$ was obtained as a function of varying DTT concentration – an identical experimental setup as the one used here. The reported error bars in Figure 5D represent standard error of the mean from each set of rates per DTT concentration ($n = 5$). The slope of r vs DTT and its standard deviation were calculated using the "LINEST" (linear least squares curve fitting routine).

Heat map generation. Heat map of disulfide reduction rates was determined through the following analysis using the programming software Interactive Data Language. Initially, the fluorescence of each pixel was averaged with its neighboring pixel intensity (2x2) for each frame of a fluorescence video and plotted into the equation $B(T) = A(0)(1 - \exp(-T \cdot A(1)))$ (where T is time/frame) for all pixels. Rate $= A(1)$ and was displayed as a heat map of rates ranging from 0.005 to 0.05.

Ensemble fluorescence measurements for calculating quenching efficiency. The fluorescence intensities of A488 and Cy3 from AuNPs functionalized protein sensors were calculated using a Biotek Synergy HT plate reader using a filter set with excitation/emission $\lambda = 485 \text{ nm}/528 \text{ nm}$ and $\lambda = 565 \text{ nm}/610 \text{ nm}$, respectively. Measurements were carried out in triplicate at a volume of 100 μl per well. To dequench the dye, volume of 50 mM KCN was added to the samples at a final concentration of 0.5 mM to dissolve away the AuNP and release the protein into solution. The fluorescence intensity of the protein sensors were subsequently measured and corrected for the quenching of the dye by KCN and AuNP filter effect as described previously⁴.

Supplementary Movie 1. Timelapse video showing the kinetics of disulfide reduction driven by the addition of 2.5 mM DTT and cellular forces. Left channel shows RCM and right channel shows fluorescence associated with unfolding of the clamped titin. Duration of the video is 6 min.

Supplementary Table 1. Values for E_a , Δx and A calculated from Arrhenius kinetic models.

Selected Publications	E _a (kJ/mol)	Δx (Å)	A (M ⁻¹ s ⁻¹)	Double-pulse force-clamp protocol	
Witta <i>et al.</i> <i>PNAS</i> , 2006	65	0.34	1 x 10 ¹²	First pulse at 130 pN for 1 sec, second pulse from 100-400 pN for 5-7 sec.	Varying [DTT] to determine <i>k</i> (<i>F</i>)
Ainavarapu <i>et al.</i> <i>JACS</i> , 2008	54	0.34	1 x 10 ¹²	First pulse at 150 pN for 0.5 sec or 180 pN for 0.2 sec, second pulse from 100-400 pN for 5 sec.	Constant [DTT] to determine E _a
Liang <i>et al.</i> <i>JACS</i> , 2011	39	0.37	1 x 10 ⁹	First pulse at 170 pN for 0.3 sec, second pulse from 100-300 pN.	Constant [DTT] to detrmine E _a and A

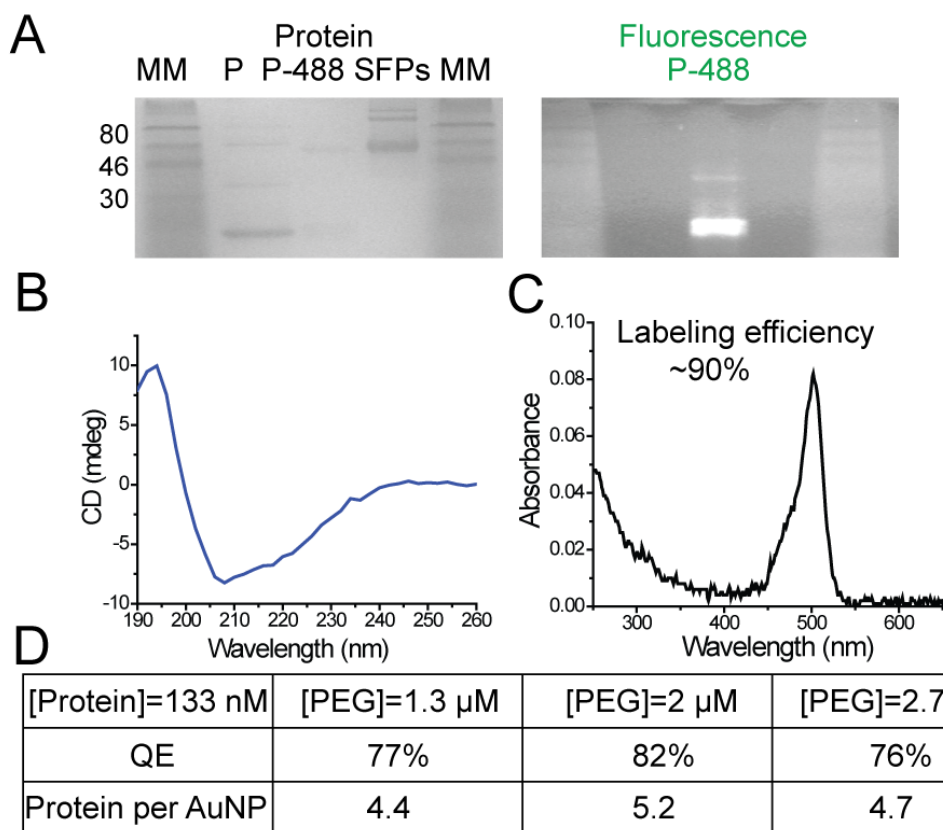


Fig. S1. Characterization of RGD-ACP(A488)-I27 MTFM sensor. (A) SDS PAGE gel (12%) stained with Coomassie Blue (left) and scanned with UV scanner (right) which indicates a high labeling efficiency of the dye with the ACP tag. From left to right: 1. Prestained protein marker (New England BioLabs); 2. RGD-ACP-I27 protein; 3. RGD-ACP-I27 labeled with CoA 488; 4. SFP synthase; 5. Prestained protein marker. (B) Far UV Circular Dichroism (CD) spectrum of unlabeled RGD-ACP-I27 (40 μM) at 37 °C which displays a mixture of α -helical (ACP) and β -sheet (I27) secondary structures suggesting that the protein remains folded at elevated temperatures. (C) Absorbance spectrum of RGD-ACP(A488)-I27. (D) Table of quenching efficiencies at different mPEG concentrations with the corresponding average number of proteins per nanoparticle.

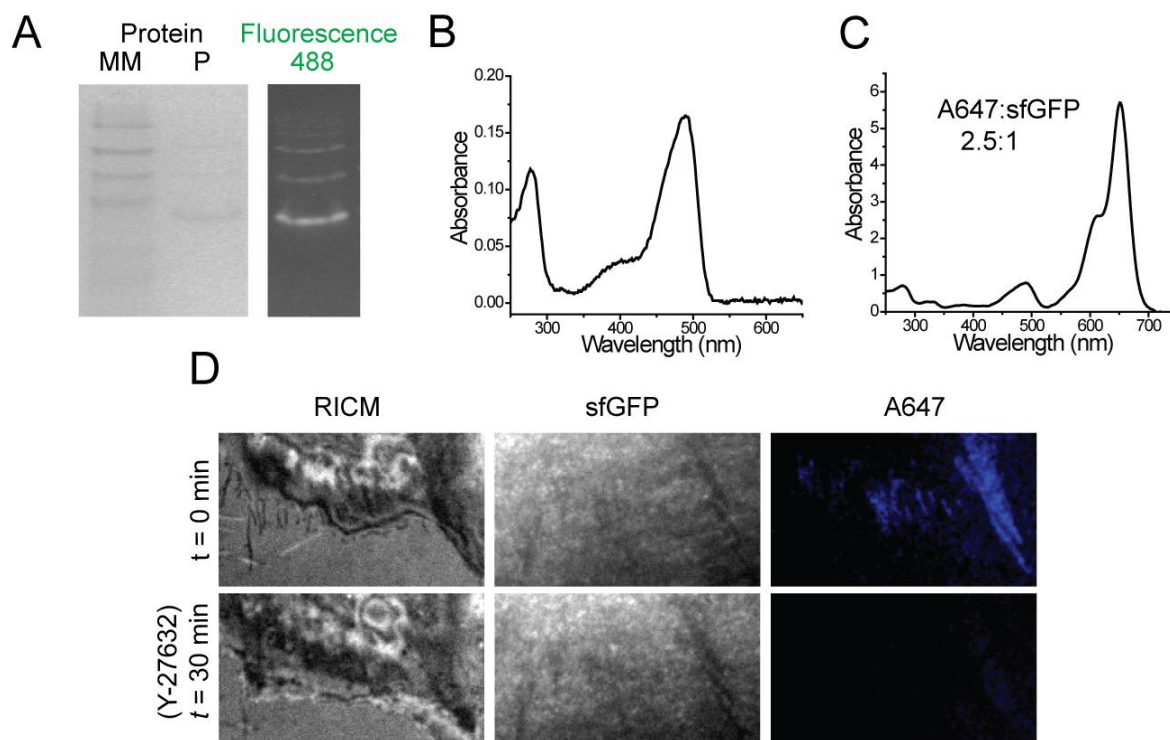


Fig. S2. Characterization of RGD-sfGFP-I27 MTFM sensor. (A) SDS PAGE gel (12%) stained with Coomassie Blue (left) and scanned with a UV scanner (right). From left to right: 1. Prestained protein marker; 2. RGD-sfGFP-I27 protein; 3. Fluorescence of RGD-sfGFP-I27 protein. (B) Absorbance spectrum of RGD-sfGFP-I27. (C) Absorbance spectrum of RGD-sfGFP-I27 randomly labeled with NHS-A647. The protein sensor was mixed with the dye at an average ratio of $\sim 1:20$ and was incubated at room temperature for 1 h. Labeled protein sensor was purified from free dye using P2 gel size exclusion beads prior to quantifying the labeling ratio by UV-Vis absorption (NanoDrop). (D) Representative RISM and fluorescence images of REF cells seeded on RGD-sfGFP-I27-A647 sensor surfaces (Protein:Dye = 1:2.5) that were treated with 40 μM of ROCK inhibitor (Y-27632) for 30 min. Fluorescence signal declined after 30 min as illustrated in the A647 channel, which indicates the loss of myosin contractility and reversibility of the sensor. However, sfGFP fluorescence was not rescued following refolding of the probe as indicated by the fluorescence images. Scale bar, 10 μm .

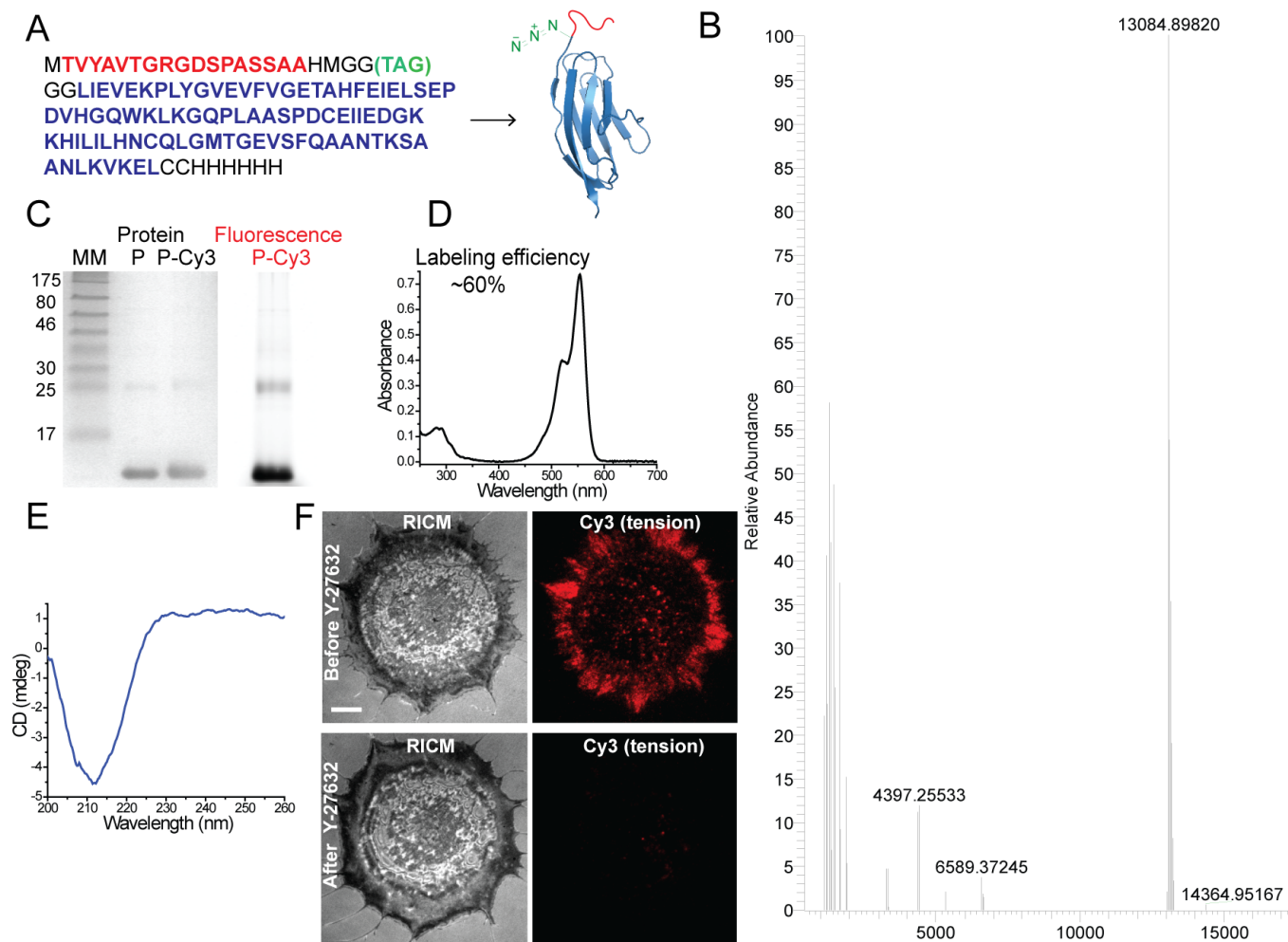


Fig. S3. Characterization of RGD-Cy3-I27 MTFM sensor. (A) Amino acid sequence of GRGDS-I27 construct including a TAG codon for *p*-azidophenylalanine incorporation (left) and crystal structure of I27 where the exact position for *p*-azidophenylalanine is added into the structure in green for clarity (right). The N terminal “GRGDS” motif is necessary for cell recognition. (B) Electrospray ionization (ESI) spectrum of the RGD-Cy3-I27 construct showing a relative abundance of 13084.9 m/z, which corresponds to the + 1 ion of the I27 MTFM sensor (calculated m/z = 13082.8). (C) SDS PAGE gel (18%) stained with Coomassie Blue (left) and scanned with a fluorescence scanner (right). From left to right: 1. Prestained protein marker; 2. RGD-I27; 3. RGD-I27 labeled with DBCO-Cy3; 4. Fluorescence of RGD-Cy3-I27 probe. (D) Absorbance spectrum of RGD-Cy3-I27. (E) Far UV Circular Dichroism (CD) spectrum of unlabeled RGD-I27 (40 μ M) at 37 $^{\circ}$ C which displays a characteristic negative band at 212 nm. This corresponds to β -sheet secondary structure of I27 and suggests that the protein is folded at elevated temperatures. (F) Representative RISM and fluorescence images of REF cells that were treated with 40 μ M of ROCK inhibitor (Y-27632) for 30 min. Fluorescence signal declined after 30 min as illustrated in the Cy3 channel indicating the loss of myosin contractility and reversibility of the RGD-Cy3-I27 sensor. Scale bar, 10 μ m.

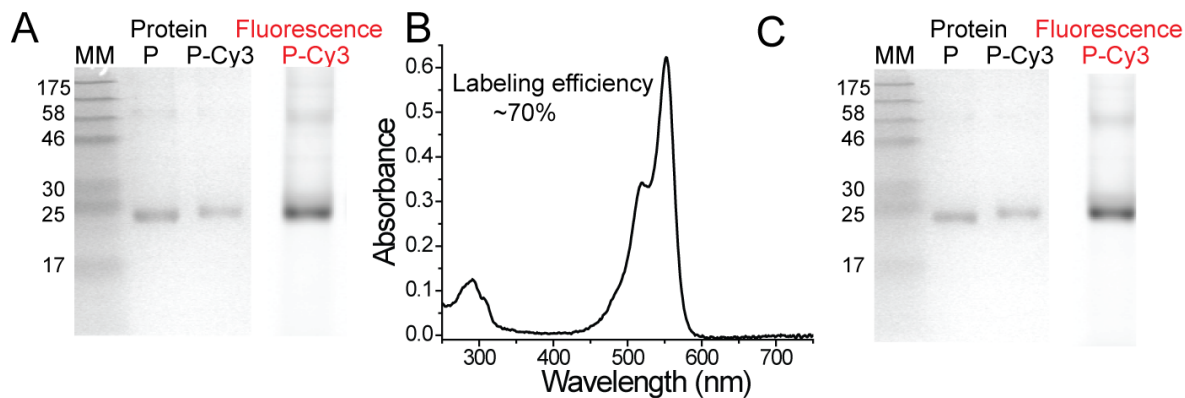


Fig. S4. Characterization of FN(9-10)-I27 and FN(9-10, RGE)-I27 MTFM sensors. (A) SDS PAGE gel (12%) stained with Coomassie Blue (left) and scanned with a fluorescence scanner (right). From left to right: 1. Prestained protein marker; 2. FN(9-10)-I27 protein; 3. FN(9-10)-I27 labeled with DBCO-Cy3; 4. Fluorescence of FN(9-10)-Cy3-I27 probe. (B) Absorbance spectrum of FN(9-10)-Cy3-I27. (C) SDS PAGE gel (12%) stained with Coomassie Blue (left) and scanned with a fluorescence scanner (right). From left to right: 1. Prestained protein marker; 2. FN(9-10, RGE)-I27 protein; 3. FN(9-10, RGE)-I27 labeled with DBCO-Cy3; 4. Fluorescence of FN(9-10, RGE)-Cy3-I27 probe.

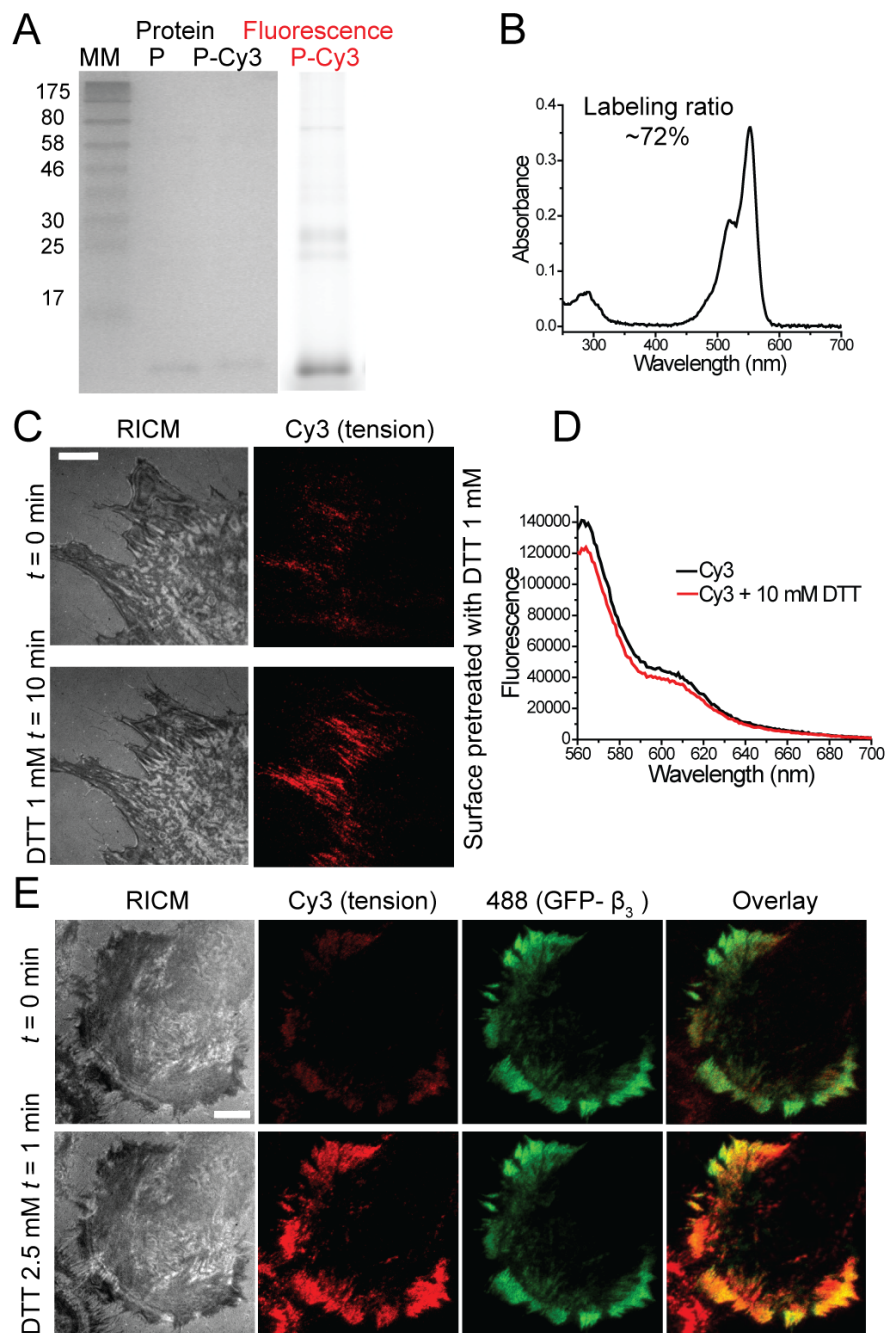


Fig. S5. Characterization of RGD-Cy3-I27_{G32C-A75C} MTFM sensor clamped with disulfide bridge. (A) SDS PAGE gel (12%) stained with Coomassie Blue (left) and scanned with a fluorescence scanner (right). From left to right: 1. Prestained protein marker; 2. RGD-I27_{G32C-A75C} protein; 3. RGD-I27_{G32C-A75C} protein labeled with DBCO-Cy3; 4. Fluorescence of RGD-Cy3-I27_{G32C-A75C} probe. (B) Absorbance spectrum of RGD-Cy3-I27_{G32C-A75C}. (C) AuNP surface functionalized with clamped RGD-Cy3-I27_{G32C-A75C} MTFM sensors was treated with 1 mM DTT for 10 min at room temperature. Surface was next rinsed with 0.1 M KH₂PO₄ and REFs were added to the surface for 1 h. Cells were then imaged in RICM and fluorescence before and after addition of 1 mM DTT. (D) Fluorescence spectrum of RGD-Cy3-I27_{G32C-A75C} protein [50 nM] treated with 10 mM DTT for 5 min to determine the effects that DTT has on the dye fluorescence. Spectrum indicates that DTT reduces the fluorescence of RGD-Cy3-I27_{G32C-A75C} by ~10% after 30 min of incubation. (E) Representative RICM and fluorescence images of REF cells expressing GFP-β₃ integrins were incubated on the clamped RGD-Cy3-I27_{G32C-A75C} sensor for 1 h and were treated with 2.5 mM DTT. Images were captured before and after 1 min of addition of DTT. Scale bar, 10 μm.

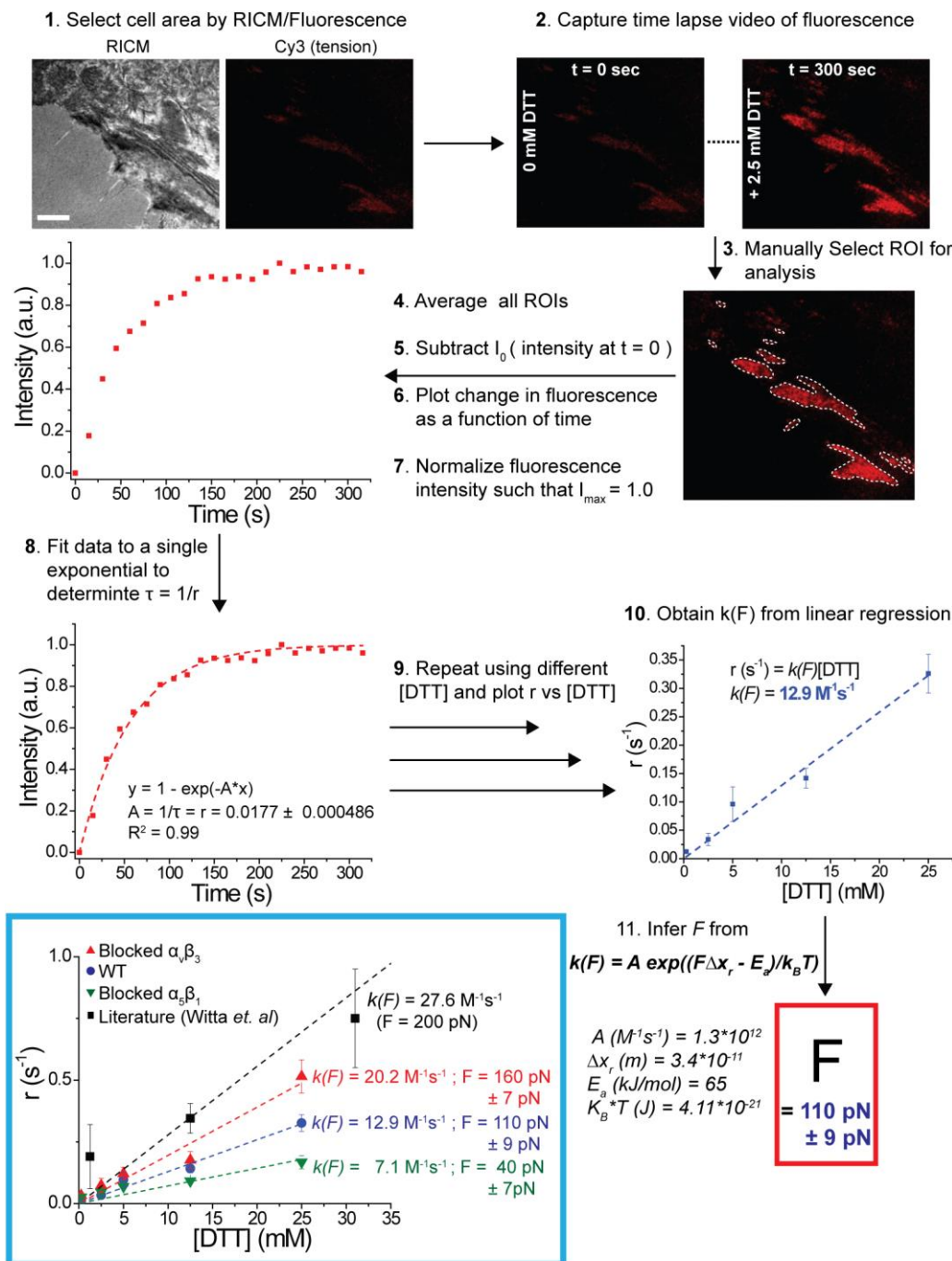


Fig. S6. Flow chart describing the analysis used for estimating integrin forces from the rate of disulfide reduction. The plot within the blue box shows a graph containing linear fits of the rate of clamped I27 reduction, $r (s^{-1})$, as a function of [DTT]. The black squares represent the data obtained from Witta *et al.*¹, while the red triangle, blue circle, and green inverted triangle represent data collected in this paper. The literature data was collected using a force clamp set at $F = 200 \text{ pN}$. This previous work included DTT concentration up to 125 mM, but the additional data points were omitted for clarity. We use the slope of the data to obtain $k(F)$, and then to infer the average force applied by cell receptors. Data was collected using REF cells (blue), cells blocked with $\alpha_5\beta_3$ (red) and $\alpha_5\beta_1$ antibodies (green).

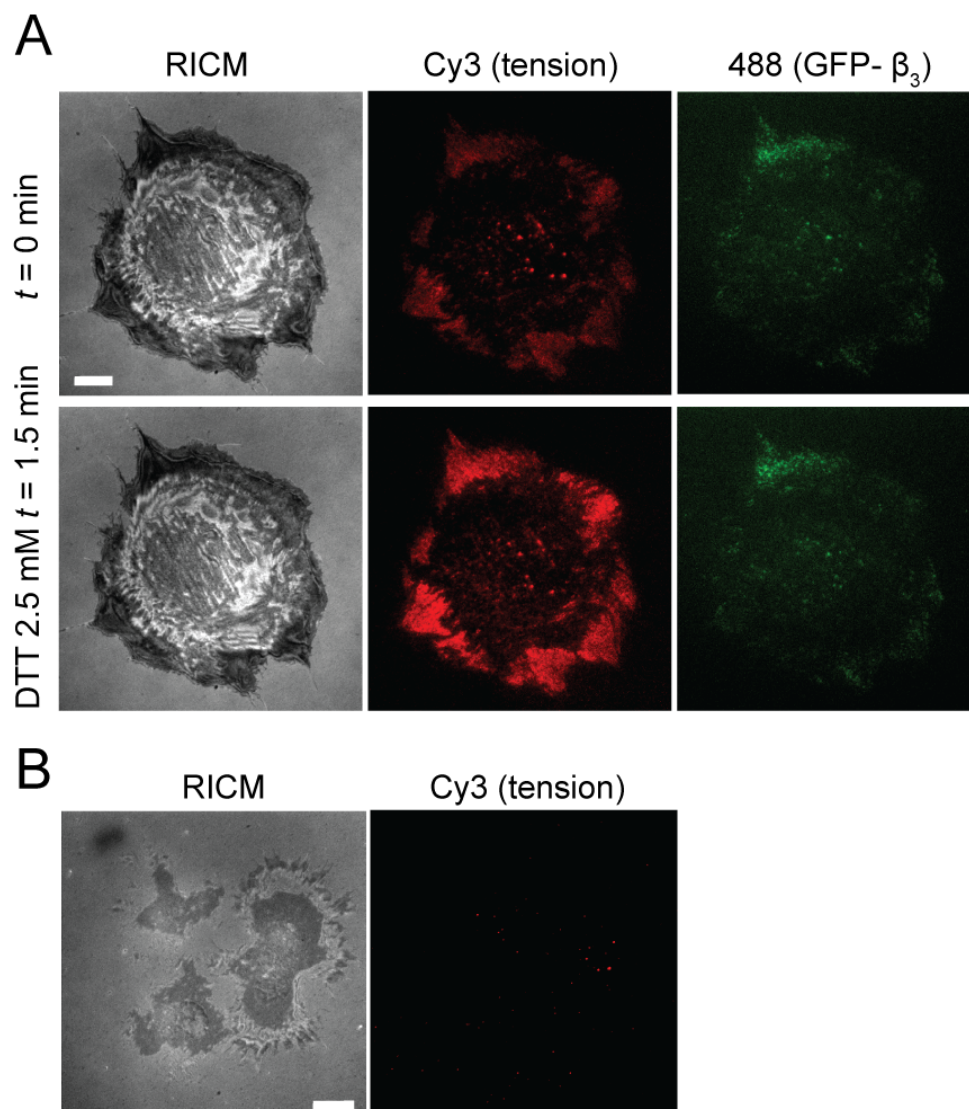
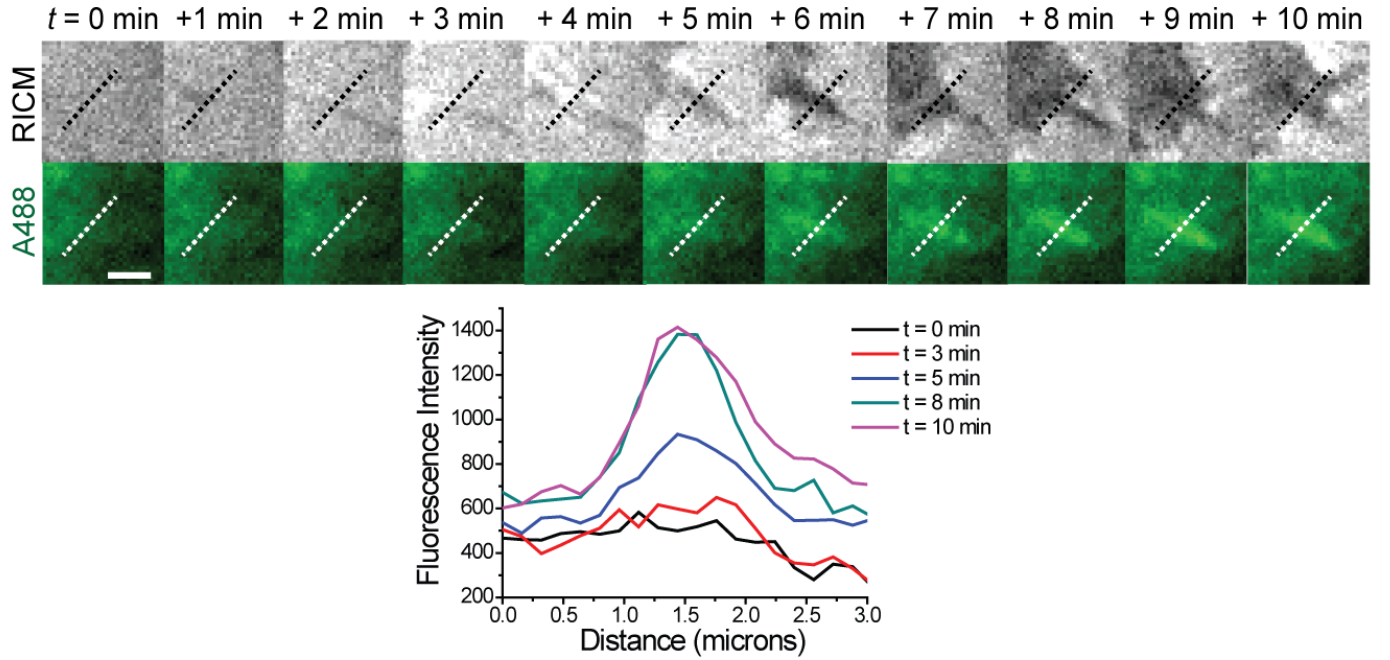


Fig. S7. Inhibition of integrin function by monoclonal antibodies specific for $\alpha_v\beta_3$ and $\alpha_5\beta_1$. (A) Representative RICM and fluorescence images of REF cells expressing GFP- β_3 integrins that were blocked with antibody against $\alpha_v\beta_3$ for 30 min and then added to a surface coated with clamped RGD-Cy3-I27_{G32C-A75C} sensors. Blocking $\alpha_v\beta_3$ integrins reveals lower GFP- β_3 localization within the cellular adhesion, which indicates the efficiency of β_3 integrin inhibition. (B) Inhibition of both $\alpha_v\beta_3$ and $\alpha_5\beta_1$ inhibits REF cells adhesion and spreading on the tension surface, which indicates that the majority of integrins employed in RGD binding are $\alpha_v\beta_3$ and $\alpha_5\beta_1$. Scale bar, 10 μ m.

Supplementary Note 1

Timelapse imaging analysis was used to determine the time difference between cell spreading and the onset of tension signal. This minimum time was then used to better estimate the minimum force required to open the I27 protein. To perform this analysis, REF cells were cultured on a RGD-ACP488-I27 probe surface for 5 min and then the timelapse movie was acquired at a rate of 1 frame per min using 300 msec exposure time in TIRFM. To determine the minimum force, we assumed that initial detectable RISM signal corresponded to the initial time point of integrin-ligand binding. We also assumed that FA maturation was instantaneous and that the receptor applied a large and constant force (force clamp) immediately following cell spreading (as determined by RISM). The constants for unfolding rate of I27 at zero force (α_0) and distance to transition state (Δx) are obtained from Carrion-Vazquez *et al.*⁵ Scale bar 2 μm .



Equations:

$$P = 1 - e^{-(\alpha)\Delta t},$$

where P is the probability of unfolding, α is a rate of unfolding and Δt is time

$$\alpha = \alpha_0 e^{(F\Delta x/k_B T)},$$

where α_0 is the unfolding rate of I27 at zero force ($3.3 \times 10^{-4} \text{ s}^{-1}$), F is the exerted force, Δx is the distance to the transition state (0.25 nm), k_B is Boltzmann's constant and T is temperature.

$$\text{at } P = 50\% \text{ and } \Delta t = 4 \text{ min, } F = 36 \text{ pN}$$

1. Wiita, A. P.; Ainavarapu, S. R.; Huang, H. H.; Fernandez, J. M., Force-dependent chemical kinetics of disulfide bond reduction observed with single-molecule techniques. *Proceedings of the National Academy of Sciences of the United States of America* **2006**, *103* (19), 7222-7.
2. Young, T. S.; Ahmad, I.; Yin, J. A.; Schultz, P. G., An enhanced system for unnatural amino acid mutagenesis in *E. coli*. *Journal of molecular biology* **2010**, *395* (2), 361-74.
3. (a) Liang, J.; Fernandez, J. M., Kinetic measurements on single-molecule disulfide bond cleavage. *Journal of the American Chemical Society* **2011**, *133* (10), 3528-34; (b) Koti Ainavarapu, S. R.; Wiita, A. P.; Dougan, L.; Uggerud, E.; Fernandez, J. M., Single-molecule force spectroscopy measurements of bond elongation during a bimolecular reaction. *Journal of the American Chemical Society* **2008**, *130* (20), 6479-87.
4. (a) Liu, Y.; Yehl, K.; Narui, Y.; Salaita, K., Tension sensing nanoparticles for mechano-imaging at the living/nonliving interface. *Journal of the American Chemical Society* **2013**, *135* (14), 5320-3; (b) Yehl, K.; Joshi, J. P.; Greene, B. L.; Dyer, R. B.; Nahta, R.; Salaita, K., Catalytic deoxyribozyme-modified nanoparticles for RNAi-independent gene regulation. *ACS nano* **2012**, *6* (10), 9150-7.
5. Carrion-Vazquez, M.; Oberhauser, A. F.; Fowler, S. B.; Marszalek, P. E.; Broedel, S. E.; Clarke, J.; Fernandez, J. M., Mechanical and chemical unfolding of a single protein: a comparison. *Proceedings of the National Academy of Sciences of the United States of America* **1999**, *96* (7), 3694-9.